Transparent ambipolar organic thin film transistors based on multilayer transparent source-drain electrodes

Article *in* Applied Physics Letters · August 2016

DOI: 10.1063/1.4960974

CITATIONS
0

READS
32

5 authors, including:

Nan Zhang
Changchun Institute of Optics, Fine Mechanic…
21 PUBLICATIONS **97** CITATIONS
SEE PROFILE

Yongsheng Hu
Changchun Institute of Optics, Fine Mechani…
17 PUBLICATIONS **59** CITATIONS
SEE PROFILE

Jie Lin
21 PUBLICATIONS **69** CITATIONS
SEE PROFILE

AIP | Applied Physics Letters

Transparent ambipolar organic thin film transistors based on multilayer transparent source-drain electrodes

Nan Zhang, Yongsheng Hu, Jie Lin, Yantao Li, and Xingyuan Liu

Citation: Applied Physics Letters **109**, 063301 (2016); doi: 10.1063/1.4960974
View online: http://dx.doi.org/10.1063/1.4960974
View Table of Contents: http://scitation.aip.org/content/aip/journal/apl/109/6?ver=pdfcov
Published by the AIP Publishing

Transparent ambipolar organic thin film transistors based on multilayer transparent source-drain electrodes

Nan Zhang, Yongsheng Hu,[a] Jie Lin, Yantao Li, and Xingyuan Liu[a]
State Key Laboratory of Luminescence and Applications, Changchun Institute of Optics, Fine Mechanics and Physics, Chinese Academy of Sciences, Changchun 130033, China

(Received 22 April 2016; accepted 2 August 2016; published online 11 August 2016)

A fabrication method for transparent ambipolar organic thin film transistors with transparent Sb_2O_3/Ag/Sb_2O_3 (SAS) source and drain electrodes has been developed. A pentacene/N,N′-ditridecylperylene-3,4,9,10-tetracarboxylic di-imide (PTCDI-C13) bilayer heterojunction is used as the active semiconductor. The electrodes are deposited by room temperature electron beam evaporation. The devices are fabricated without damaging the active layers. The SAS electrodes have high transmittance (82.5%) and low sheet resistance (8 Ω/sq). High performance devices with hole and electron mobilities of 0.3 cm^2/V s and 0.027 cm^2/V s, respectively, and average visible range transmittance of 72% were obtained. These transistors have potential for transparent logic integrated circuit applications. *Published by AIP Publishing*. [http://dx.doi.org/10.1063/1.4960974]

Over the past decade, transparent thin film transistors (TFTs) have received increasing attention because of their potential for applications including transparent logic circuits and organic light emitting diode displays.[1,2] Recently, there has been great progress in the development of transparent TFTs, which are showing high performance and are highly practical.[2–4] However, despite the rapid advancements in transparent TFTs,[2,3,5] most of them are still unipolar devices, which generally operate as n-channel or p-channel transistors. The ideal low power way to use these transistors is to realize complementary circuits like silicon-based integrated circuits (ICs).[6–8] To date, hole transport has been difficult in oxide semiconductors because of small band dispersion and the deep energy levels that result from the valence band maximum.[9] Therefore, high performance oxide TFTs almost all operate in n-channel mode, and there are few p-channel or ambipolar oxide TFTs. The studies on transparent ambipolar oxide TFTs have shown that the performance of these devices is even lower than that of ambipolar organic TFTs.[10,11] Also, the oxide TFT fabrication process is more complex than that of organic TFTs in actual production, which means high costs and low yield. With regard to organic TFTs, because instability of n-type organic semiconductor materials and energy level mismatch between the organic active layer and source-drain electrodes that hinder the development of n-channel or ambipolar transparent organic TFTs, most of transparent organic TFTs are p-channel devices whose channel carrier is hole. There have been few reports about n-channel or ambipolar transparent organic TFTs. In transparent ambipolar organic TFTs, poly(ethylenedioxythiophene):poly (styrenesulfonate) (PEDOT:PSS) was generally used for the source-drain electrodes in the transparent device structure.[12] However, those transparent ambipolar organic TFTs based on PEDOT:PSS showed poor device performance,[12,13] which were difficult to be applied in logic integrated circuits. Until now, the fabrication processes and properties of transparent source-drain electrodes for transparent ambipolar organic TFTs have been far from satisfactory.

According to previous studies, when a highly reflective metal layer is inserted between two dielectric layers with high refractive indexes, the resulting dielectric-metal-dielectric (DMD) structure can achieve enhanced transmittance in a selective region via the interference effect.[14,15] DMD multilayers have been used as transparent anodes in bottom-emitting organic light-emitting diodes (OLEDs),[16] with optical properties that are comparable to those of indium tin oxide (ITO)-based OLEDs. Hong *et al*. demonstrated that a thermally evaporated WO_3/Ag/WO_3 transparent top cathode structure enhanced the optical properties of top-emitting OLEDs.[17] Also, flexible polymer photovoltaic cells using SiO_2/WO_3/Ag/WO_3 (SWAW) transparent electrode structures have been reported, and the flexible SWAW transparent electrodes have excellent optical-electrical properties, strong adhesion, and good stability.[18]

In this work, we have developed high performance transparent ambipolar organic TFTs based on transparent source and drain electrodes with Sb_2O_3/Ag/Sb_2O_3 (SAS) DMD structures. A pentacene/N,N′-ditridecylperylene-3,4,9,10-tetracarboxylic di-imide (PTCDI-C13) bilayer heterojunction was used as the active semiconductor to realize these ambipolar organic TFTs. The SAS electrode is deposited at room temperature by electron beam thermal evaporation, which is an organic device-compatible fabrication process with causing little damage to the active organic layer. High transmittance and low sheet resistance can be obtained when the SAS electrodes are deposited on glass substrates. Transparent ambipolar organic TFTs show high carrier mobilities of 0.3 cm^2/V s and 0.027 cm^2/V s for holes and electrons, respectively, and a visible range transmittance of 72%.

The SAS transparent electrodes were deposited on glass substrates that had been ultrasonically cleaned (with acetone, ethanol, and de-ionized water). Sb_2O_3, Ag, and Sb_2O_3 films were prepared under a vacuum pressure of 2×10^{-3} Pa and were deposited sequentially at room temperature by electron beam evaporation. The Sb_2O_3 and Ag evaporation rates, which

[a]Electronic addresses: huyongsheng@ciomp.ac.cn and liuxy@ciomp.ac.cn

were monitored *in situ* using a thin film deposition controller, were 0.2 nm/s and 1 nm/s, respectively. Pentacene and PTCDI-C13 were purchased from Lumtech and Sigma-Aldrich, respectively. Poly-4-vinylphenol (PVP), poly(melamine-co-formaldehyde), and propylene glycol monomethyl ether acetate (PGMEA) were also purchased from Sigma-Aldrich. These materials were all used without further treatment. The ITO gate electrodes were patterned by photolithography and wet etching. The ITO glass substrates were then ultrasonically cleaned with acetone, ethanol, and deionized water in sequence. Then, PVP, serving as the organic dielectric layer, was prepared by spin coating of PVP and poly(melamine-co-formaldehyde) methylated in PGMEA. The PVP layer was annealed at 180 °C for 2 h under an ambient air environment. The PVP layer thickness was 400 nm. Layers of 12-nm-thick pentacene and 40-nm-thick PTCDI-C13 were subsequently thermally evaporated on the substrate at a base pressure of 1.5×10^{-4} Pa. The evaporation rates of pentacene and PTCDI-C13 were 0.2 Å/s and 0.5 Å/s, respectively. The work functions were investigated with a KP Technology Ambient Kelvin probe system package.

To obtain SAS electrodes with high optical transmittance, we fabricated the SAS electrodes with different structures. The transmittance spectra of SAS electrodes with different Sb_2O_3 and Ag layer thicknesses are shown in Figure 1(a). The data also show that the average visible range transmittance ($\lambda = 400$–750 nm) of the SAS electrodes can be up to 82.5% with an electrode layer thickness structure of 35 nm/12 nm/40 nm. Based on these results, we then investigated the correlation between the sheet resistance and the transmittance. Figure 1(b) shows the change in measured sheet resistance and transmittance (at $\lambda = 550$ nm) of SAS electrodes as a function of Ag thickness. When the Ag thickness is in the 8–12 nm range, the SAS electrode has higher transmittance than in any other range. For Ag thicknesses of over 16 nm, lower transmittance values result from the high reflectance of the Ag layer.[17] The SAS sheet resistance decreases dramatically, from 40 Ω/sq to 3.5 Ω/sq, with increasing Ag thickness. This result indicates that the Ag thickness determines the electrical properties of the SAS electrodes. SAS electrodes with Ag layer thickness of less than 8 nm show higher sheet resistance because of the discontinuous Ag island growth.[15,18] From the above experimental results, we can confirm that the SAS electrodes (with layer thicknesses of 35 nm/12 nm/40 nm, average transmittance of 82.5% and sheet resistance of 8 Ω/sq) have competitive properties when compared with other transparent electrode structures.

The transmittance spectra of the device (as the number of individual layers increased in order) is shown in Figure 1(c). The transmittance of the samples between 400 nm and 800 nm decreased slightly when the individual layers were stacked from the ITO gate electrode layer to the active layers (pentacene and PTCDI-C13) in sequence. The absorption peak that was observed near 670 nm after deposition of the pentacene and PTCDI-C13 layers is related to the orbital gap of pentacene between the highest occupied molecular orbital and the lowest unoccupied molecular orbital,[19] and the other spectral feature (near 520 nm) corresponds to the energy gap of PTCDI-C13.[20] The ambipolar organic TFTs with SAS electrodes exhibit an average transmittance of 72% in the visible range (from 400 nm to 750 nm), which is lower than the transmittance of 80% achieved in devices without SAS electrodes. The gap is a result of the red light absorption of SAS electrodes and the refractive index mismatch among the functional layers (including the gate electrode, the insulator layer, the active layer, and the source-drain electrodes). However, the average transmittance of the device is 72% and the devices will become more transparent as we further improve the structures.

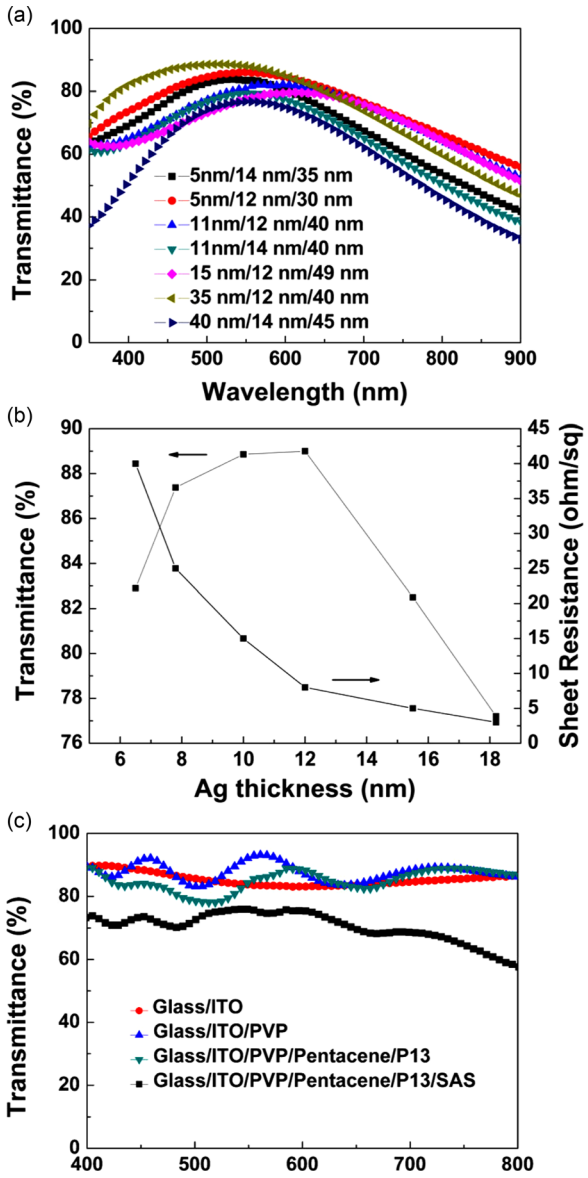

FIG. 1. (a) Transmittance spectra of SAS electrodes with different Sb_2O_3 and Ag thicknesses. (b) Transmittance at a wavelength of 550 nm and sheet resistance of the SAS electrodes as a function of the Ag thickness. The structure of the electrodes is 35 nm/x (Ag thickness) nm/40 nm. (c) Transmittance spectra of the transparent device with increased stacking of the layers from ITO to SAS.

Figures 2(a) and 2(b) show the p- and n-type output characteristic curves for the ambipolar organic TFTs with SAS electrodes, respectively. The output curves indicate that the devices are in the ambipolar operation mode and that the I–V behavior of the p-type is better than that of the n-type. To switch the polarities of the TFTs, gate voltages of more

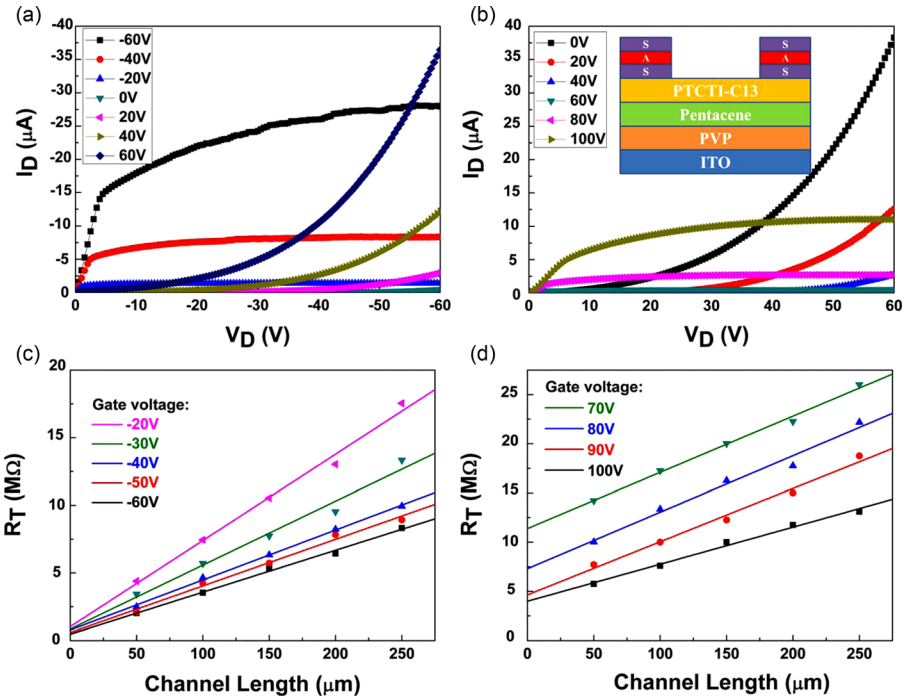

FIG. 2. Output characteristic curves of (a) p-type and (b) n-type operations in transparent ambipolar organic TFTs with the applied gate voltage (a) from −60 V to 60 V and (b) from 0 V to 100 V. TLM-estimated data of (c) the negative gate voltage from −60 V to −20 V, and (d) the positive gate voltage from 70 V to 100 V. Inset: a schematic of the transparent ambipolar organic TFTs with SAS source-drain electrodes.

than 0 V and 60 V are required (see Figures 2(a) and 2(b), respectively). The interface contact resistance between the transparent electrodes and the organic semiconductors is an important factor that dominates the performance of transparent organic TFTs. The contact resistance can be calculated using the transmission-line method (TLM).[21,22] Figures 2(c) and 2(d) show a plot of R_T as a function of channel length L. The contact resistance can be obtained from the intercepts of linear fits to the data. Based on the results shown in Figures 2(c) and 2(d), we find that the contact resistance at negative gate voltage is higher than that at positive gate voltage, which indicates that the hole injection barrier is more lower than the electron injection barrier between the transparent electrodes and organic semiconductors. These results suggest that hole mobility μ_h of the transparent ambipolar transistors is higher than the electron mobility μ_e.

The transfer characteristics of the devices are shown in Figures 3(a) and 3(b). We list the electrical parameters of transparent ambipolar organic TFTs with SAS source-drain electrodes in Table I. Based on our calculations, we found that the electron mobility of the ambipolar transistors was lower than the hole mobility. Similar results can be found in the literature.[12,23] The work function of the SAS structure is −5.1 eV (see the inset of Figure 3(c)). There is an electron injection barrier at the PTCDI-C13/SAS interface of 1.7 eV, while the hole barrier between pentacene and SAS is only 0.1 eV. According to previous studies, when the electron injection barrier reached 1.5 eV, ambipolar organic transistors showed poor n-type behavior.[12] Therefore, the larger electron injection barrier leads to lower field-effect mobility for electrons than for holes. The high and balance carrier mobilities are difficult to achieve at the same time in transparent ambipolar transistors. So far, there are no ideal reports about that a better balance between the energy level of organic semiconductor materials (n-type and p-type in one transistor) and the work function of transparent electrodes

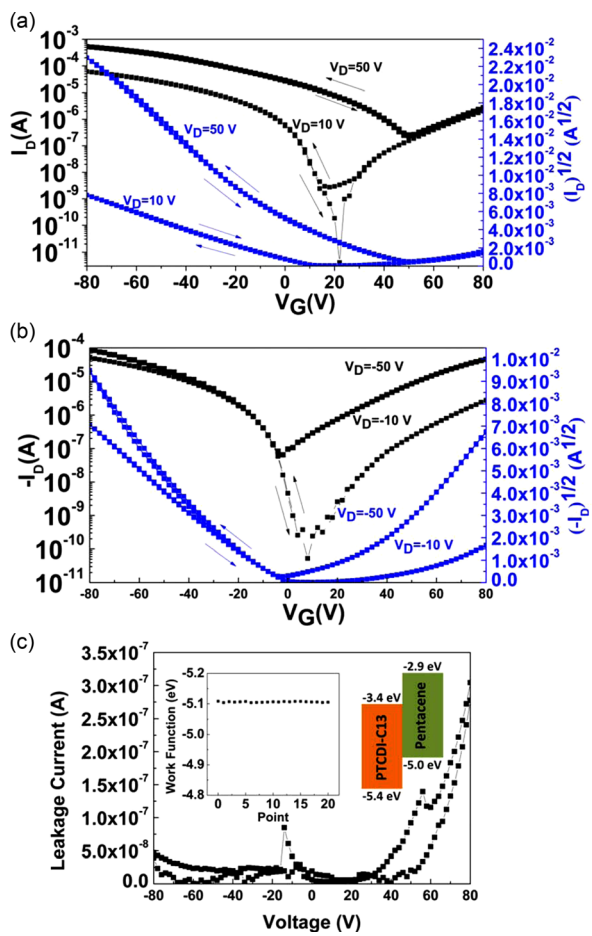

FIG. 3. Transfer characteristics of transparent ambipolar organic TFTs with SAS source-drain electrodes at drain voltage (a) $V_D = 10$ V, $V_D = 50$ V, and (b) $V_D = -10$ V, $V_D = -50$ V. (c) The leakage current versus voltage. Inset: Work functions of the SAS electrodes and energy diagram of the pentacene/PTCDI-C13 bilayer heterojunction.

TABLE I. The electrical parameters of transparent ambipolar organic TFTs at drain voltage ±10 V and ±50 V: electron mobility μ_e, hole mobility μ_h, threshold voltage V_T, I_{on}/I_{off}, subthreshold swing. The number of the devices is 25.

V_D (V)	Carrier transport region	Electron mobility μ_e ($cm^2/V\,s$)	Hole mobility μ_h ($cm^2/V\,s$)	Threshold voltage V_T (V)	I_{on}/I_{off}	Subthreshold swing (V/dec)
10	n type	0.014 ± 0.002	…	49 ± 4	1×10^5–1×10^6	12 ± 2
10	p type	…	0.06 ± 0.01	−0.35 ± 0.1	1×10^6–1×10^7	10 ± 2
50	n type	0.024 ± 0.003	…	53 ± 2	10–20	27 ± 2
50	p type	…	0.28 ± 0.02	30 ± 2	1×10^2–1×10^3	20 ± 1
−10	n type	0.017 ± 0.003	…	−49 ± 3	1×10^5–1×10^6	12 ± 1
−10	p type	…	0.066 ± 0.005	−10±1	1×10^6–1×10^7	6 ± 1
−50	n type	0.12 ± 0.02	…	31 ± 4	1×10^3–1×10^4	23 ± 2
−50	p type	…	0.2 ± 0.03	27 ± 3	1×10^3–1×10^4	10 ± 1

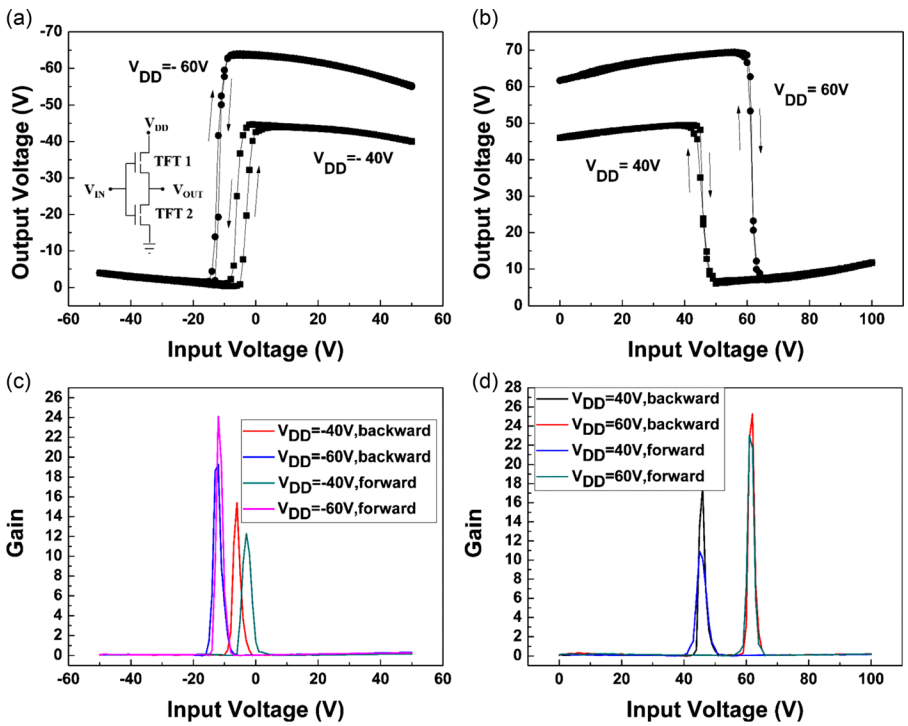

FIG. 4. The voltage-transfer characteristics of the inverter at the supply voltages (V_{DD}) of (a) −40 V, −60 V and (b) 40 V and 60 V. (c) and (d) show the corresponding voltage gains of the inverter. The inset shows the circuit diagram of the inverter.

with opportune fabrication processes and good photoelectric properties. Thus, the SAS source-drain electrodes have low sheet resistance, high transmittance, and can be deposited without damaging the active layer, which contribute to the high performance of the transparent ambipolar organic TFTs, and show great potential for improving the performance of transparent devices.

The transparent ambipolar TFTs have been applied in the inverter. Figures 4(a) and 4(b) show the high switching speeds with sharp inversions and little hysteresis at the supply voltages (V_{DD}) of ±40 V and ±60 V, and the maximum gain is greater than 25. Therefore, the inverter exhibits better electrical parameters than that of other inverters based on unipolar p- and n-type OTFTs. These results indicate that employing ambipolar TFTs is better than using two unipolar TFTs.[24,25]

In summary, high performance transparent ambipolar organic TFTs using SAS multilayers as source and drain electrodes have been developed. The SAS electrodes are deposited at room temperature by electron beam thermal evaporation, causing little damage to the active organic layers, and have high average transmittance of 82.5% and low sheet resistance of 8 Ω/sq. The hole and electron mobilities of the transparent ambipolar organic TFTs are up to 0.3 $cm^2/V\,s$ and 0.027 $cm^2/V\,s$, respectively. The average visible range transmittance of the transparent device is 72%. Furthermore, we obtained the inverters based on transparent ambipolar organic TFTs, which exhibit better electrical parameters than those of other inverters based on unipolar p- and n-type organic TFTs. These results indicate that the DMD structure of SAS is an excellent choice for source-drain electrodes for transparent ambipolar TFTs, and that these TFTs have potential for use in transparent logic ICs.

This work was supported by the CAS Innovation Program, and the National Natural Science Foundation of China through Grant No. 6140031454, and Project supported by State Key Laboratory of Luminescence and Applications.

[1]M. S. Oh, K. Lee, K. H. Lee, S. H. Cha, J. M. Choi, B. H. Lee, M. M. Sung, and S. Im, Adv. Funct. Mater. **19**(5), 726 (2009).
[2]J. Zhang, C. Wang, and C. Zhou, ACS Nano **6**(8), 7412 (2012).

[3]X. Qian, T. Wang, and D. Yan, Org. Electron. **14**(4), 1052 (2013).
[4]H. Moon, H. Cho, M. Kim, K. Takimiya, and S. Yoo, Adv. Mater. **26**(19), 3105 (2014).
[5]H. Ohta, T. Kambayashi, K. Nomura, M. Hirano, K. Ishikawa, H. Takezoe, and H. Hosono, Adv. Mater. **16**(4), 312 (2004).
[6]J. Zaumseil and H. Sirringhaus, Chem. Rev. **107**(4), 1296 (2007).
[7]Y. Zhao, Y. Guo, and Y. Liu, Adv. Mater. **25**(38), 5372 (2013).
[8]S. Z. Bisri, C. Piliego, J. Gao, and M. A. Loi, Adv. Mater. **26**(8), 1176 (2014).
[9]H. Hosono, Y. Ogo, H. Yanagi, and T. Kamiya, Electrochem. Solid-State Lett. **14**(1), H13 (2011).
[10]K. Nomura, T. Kamiya, and H. Hosono, Adv. Mater. **23**(30), 3431 (2011).
[11]Y. Hu, N. Zhang, J. Lin, L. Qin, and X. Liu, Appl. Phys. Express. **5**(9), 095601 (2012).
[12]P. Cosseddu, A. Bonfiglio, I. Salzmann, J. Rabe, and N. Koch, Org. Electron. **9**(2), 191 (2008).
[13]P. Cosseddu and A. Bonfiglio, Appl. Phys. Lett. **97**(20), 203305 (2010).
[14]Y.-S. Park, H.-K. Park, J.-A. Jeong, H.-K. Kim, K.-H. Choi, S.-I. Na, and D.-Y. Kim, J. Electrochem. Soc. **156**(7), H588 (2009).
[15]C. Song, H. Chen, Y. Fan, J. Luo, X. Guo, and X. Liu, Appl. Phys. Express. **5**(4), 041102 (2012).
[16]H. Cho, C. Yun, J.-W. Park, and S. Yoo, Org. Electron. **10**(6), 1163 (2009).
[17]K. Hong, K. Kim, S. Kim, I. Lee, H. Cho, S. Yoo, H. W. Choi, N.-Y. Lee, Y.-H. Tak, and J.-L. Lee, J. Phys. Chem. C **115**(8), 3453 (2011).
[18]X. Guo, J. Lin, H. Chen, X. Zhang, Y. Fan, J. Luo, and X. Liu, J. Mater. Chem. **22**(33), 17176 (2012).
[19]J.-M. Choi, D. Hwang, J. H. Kim, and S. Im, Appl. Phys. Lett. **86**(12), 123505 (2005).
[20]A. S. Wan, J. P. Long, G. Kushto, and A. J. Mäkinen, Chem. Phys. Lett. **463**(1), 72 (2008).
[21]T. Minari, T. Miyadera, K. Tsukagoshi, Y. Aoyagi, and H. Ito, Appl. Phys. Lett. **91**(5), 053508 (2007).
[22]M. Imakawa, K. Sawabe, Y. Yomogida, Y. Iwasa, and T. Takenobu, Appl. Phys. Lett. **99**(23), 233301 (2011).
[23]Y. Hu, Q. Lu, H. Li, N. Zhang, and X. Liu, Appl. Phys. Express **6**(5), 051602 (2013).
[24]L. Basirico, P. Cosseddu, B. Fraboni, and A. Bonfiglio, Thin Solid Films **520**(4), 1291 (2011).
[25]J.-D. Oh, J.-W. Kim, D.-K. Kim, and J.-H. Choi, Org. Electron. **30**, 131 (2016).